https://doi.org/10.5194/egusphere-2026-622
Preprint. Discussion started: 12 February 2026


# Planktonic foraminifera Iodine/Calcium ratio: is it a proxy for dissolved oxygen in the ocean?

Vincent Guarinos[1*], Kazuyo Tachikawa[1], Marta Garcia[1], Giuseppe Siani[2], Marie Revel[3], Hartmut Schulz[4], Francisco Sierro[5], Thomas Chalk[1]

[1]Aix Marseille Univ, CNRS, IRD, INRAE, Coll France, CEREGE, Aix-en-Provence, France.

[2]Laboratoire de Géosciences Paris-Saclay (GEOPS), CNRS, Paris Saclay, France.

[3]Université de la Cote d'Azur, CNRS, OCA, IRD, Geoazur, Valbonne, France.

[4]Department of Geosciences, University of Tübingen, Tübingen, Germany.

[5]Dept. de Geología, Univ. de Salamanca, Plaza de los Caídos s/n, 37008, Salamanca, Spain

*Correspondence to*: Guarinos Vincent (guarinos@cerege.fr)

**Abstract**

Direct observations indicate a declining trend in ocean oxygen concentrations, which is not quantitatively captured by models. The complexity of oxygenation variability, linked to both physical and biochemical parameters, must be investigated across different modern climate contexts. Foraminiferal iodine-to-calcium (I/Ca) ratios have emerged as a proxy for subsurface oxygen concentrations although its capacity for quantitative reconstructions remains to be elucidated. We provide a new database of modern foraminiferal I/Ca, including the first results from the Mediterranean Sea and new samples in the Arabian Sea together with the parameters of biochemistry (nutrient concentration, pH, chlorophyll, oxygen, net primary productivity), physical and geographical (temperature, salinity, latitude, distance from the coast, water depths) and diagenesis potential (depth in core, sediment age) to better understand the proxy behaviour. Considering the strong spatiotemporal variability in dissolved oxygen in subsurface ocean, we propose to use statistically robust 25$^{th}$ percentile of oxygen concentration (p25 [$O_2$]) instead of minimum concentration in the upper 500 m in the water column. Our results affirm that oxygen concentration is the primary driver of foraminiferal I/Ca and we propose a new calibration equation of foraminiferal I/Ca against p25 [$O_2$]. Based on a new database, we identify a complex relationship between p25 [$O_2$] and iodine speciation, which is one of the main sources of scatter. A comparison with synthetic calcite reveals that planktonic foraminiferal tests can incorporate either more or less iodate at high p25 [$O_2$] than abiotic calcite, probably due to "vital effects". The Mediterranean Sea samples present a wide range from low to high I/Ca (0.6 to 6.9 µmol/mol) in well-oxygenated water, which cannot be explained solely by authigenic calcite precipitation. Our results highlight the complex behaviour of the I/Ca proxy, while reinforcing its semi-quantitative reconstruction in palaeoceanography.

## Introduction

https://doi.org/10.5194/egusphere-2026-622
Preprint. Discussion started: 12 February 2026


Oxygen concentration [$O_2$] in the global ocean is decreasing, and the decline is highly influenced by warming patterns induced by global climate change (Oschlies et al., 2018). Future oxygenation change is difficult to predict as it depends on various parameters. Dissolved oxygen depletion can be related to changes in solubility with seawater temperature, generally decreasing ventilation of water masses (Oschlies et al., 2017), and/or through biological productivity triggered oxygen consumption in the ocean, especially in the subsurface, where the productivity and remineralisation are at a maximum. Models can currently only explain about half the observed oxygen depletion (Bopp et al., 2013; Frölicher et al., 2016) and thus a proxy for subsurface oxygen content is highly sought to study longer variability under different climate conditions.

The iodine to calcium ratios (I/Ca) from planktonic foraminifera tests have been investigated and used as a proxy for subsurface/intermediate depth minimum oxygen concentration (Lu et al., 2010, 2016, 2020; Winkelbauer et al., 2021; Hess et al., 2025; Zhou et al., 2014, 2022; Hoogakker et al., 2024) as inorganic iodine speciation depends on redox potential, which is mainly controlled by oxygen content (Luther, 2023). Severe oxygen depletion, less than 1 nM of oxygen, will chemo-dynamically trigger iodate reduction to iodide ($I^-$) (Luther, 2023). In oxygenated water, iodine is mainly in its oxidized form, iodate ($IO_3^-$) (Chance et al., 2014, 2019). Iodide, the reduced form of inorganic iodine can also be found in small concentrations near surface because of biological iodate uptake and iodide release during phytoplankton growth (Hepach et al., 2020). In hypoxic and anoxic waters, iodide is the major iodine species, thought to increase as iodate is reduced. The reduction reaction takes place under short time scales, from days to weeks (Chance et al., 2010) whereas the full (re)oxidation of iodide back to iodate has been reported to take place from several weeks to several months (Wadley et al., 2020). Total inorganic iodine in oxygenated water typically ranges between 400 and 500 nM, corresponding to a variability of about 20% (Chance et al., 2010). Iodine is also present as organically bound iodine, primarily in the form of dissolved organic iodine. In the open ocean, it is typically about 5% of total dissolved iodine, but this proportion can increase to up to ~20% in coastal areas due to interaction with higher concentrations of dissolved organic matter (Jones et al., 2024). Iodate is assumed to be the only iodine species to be incorporated to foraminiferal calcite tests as a substitute to carbonate ion (Feng and Redfern, 2018; Lu et al., 2010; Podder et al., 2017). The processes and kinetics of the chemical reactions in the water column, as well as its incorporation mechanisms into biologically mediated calcite are still poorly understood (Luther, 2023).

Calibration of the I/Ca–$O_2$ proxy was first focused on the quantitative reconstruction of subsurface oxygen concentration as synthetic calcite showed linear incorporation of iodate depending on its concentration (Lu et al., 2010). Later, foraminiferal core-top calibrations started to relate the I/Ca ratio in respect with minimum oxygen from 0–500 m in the water column, considering a tight relationship between the minimum oxygen concentration and surface water iodate concentration (Lu et al., 2016). The proxy was thus proposed as a semi-quantitative tool with a threshold I/Ca value of 2.5 µmol/mol that corresponds to [$O_2$] <70 µmol/kg (Lu et al., 2016). Data from the Southeast Atlantic including sites close to the Benguela upwelling system highlighted the possibility of low I/Ca in apparently oxygenated water (Lu et al., 2020). The minimum oxygen values of the study region were highly spatially variable and the use of oxygen data at higher resolution (0.25°) reduced the number data points with low I/Ca under high oxygenation condition (Lu et al., 2020). However, substantial scatter remains in the relationship between foraminiferal I/Ca and minimum oxygen concentration that is characterised by two broad domains: oxygen depleted waters (I/Ca <2.5 µmol/mol) and oxygenated water (I/Ca >4 µmol/mol). Nilsson-Kerr et al. (2025) expanded the I/Ca–$O_2$ core top calibration dataset with measurements from regions with low subsurface

https://doi.org/10.5194/egusphere-2026-622
Preprint. Discussion started: 12 February 2026


$O_2$, confirming the presence of significant scatter. Hess et al. (2025) proposed that I/Ca dispersion is linked with the different iodate concentrations at different foraminiferal calcification depths. Scattering could then be reduced by using Mg/Ca ratios in the foraminifera, a proxy for temperature that estimates their calcification depth. Although they showed that I/Ca varies predictably based on iodate concentration and water depth, substantial dispersion still persists and the effect of calcification depth cannot explain all the results.

Moreover, low I/Ca from plankton tow in highly oxygenated waters have been measured (Winkelbauer et al., 2023). It was suggested that iodine is incorporated during particle sinking and could explain those low values, thus challenging the use of the proxy for subsurface oxygenation, an interpretation that has not yet been further interrogated. Besides, given the lack of knowledge on the underlying mechanism, application of this proxy needs caveating when carried out for samples from coastal shelves and restricted basins where the mixing with open ocean water is not efficient (Hess et al., 2025).

The previous studies have mostly focused on trying to reduce scattering by investigating the Y-axis (I/Ca), but the definition of X-axis (oxygen concentration) has not been treated systematically, despite its importance (Lu et al., 2020). Some studies suggest that the complexity of iodine speciation and its coupling with dissolved oxygen is responsible for the observed data scatter (Hess et al., 2025; Nilsson-Kerr et al., 2025). However, the systematic study with a large number of data focusing on both the definition of minimum dissolved oxygen concentration and iodine speciation has not yet been realised.

We aim to determine whether the definition of "oxygen concentration" can help to better calibrate the proxy, and further investigate the possible reasons for foraminiferal I/Ca data scattering. We also examine if the proxy can be used in a semi-enclosed basin, the Mediterranean Sea. In this paper, our approach is to (1) propose a statistically robust definition for minimum $O_2$, (2) investigate the coupling between iodine speciation and dissolved oxygen as a potential control for foraminiferal I/Ca scattering (3) examine the differences in iodine incorporation between foraminiferal and abiotic calcite, and (4) evaluate the influence of authigenic carbonate precipitation on foraminiferal I/Ca under high alkalinity conditions.

## 1 Material and Methods

### 1.1 Material

In this study we present core top planktonic foraminiferal I/Ca from 7 locations including 5 from the Mediterranean region (Fig. 1b). Core MD99-2341 (577 mbsl) from Gulf of Cadiz together with ODP Site 977 (1984 mbsl) from Alboran Sea are selected to characterise the Atlantic inflow signature. MD04-2797 (771 mbsl) is located next to the Strait of Sicily, and is used to indicate mixing ratio at the connection between the Western and Eastern Mediterranean basins. SL95 (1390 mbsl), in the Gulf of Sirte, is thought to represent the southern part of the Ionian Sea. Core MD04-2724 (1659 mbsl) has been recovered in the deep Nile delta and it is the easternmost core of this study. MD90-917 (1010 mbsl), was recovered in the Adriatic Sea, where the Eastern Mediterranean deep water is formed and corresponds to a well oxygenated area. The two other cores MD04-2873 (2196 mbsl) and MD04-2876 (828 mbsl) were recovered in the Pakistan margin, one below the Oxygen Minimum Zone (OMZ), and the other inside it, respectively (Fig. 1c). They are selected in order to identify any impact of the bottom water oxygenation state on I/Ca ratios.

https://doi.org/10.5194/egusphere-2026-622
Preprint. Discussion started: 12 February 2026


We present the first measurements from 2 new cores, SL95 and MD04-2724. The core tops were dated to 1,835 ± 30 (1sd, at 0–1 cm) and 5,515 ± 30 radiocarbon years BP (1sd, at 0–1cm) respectively.

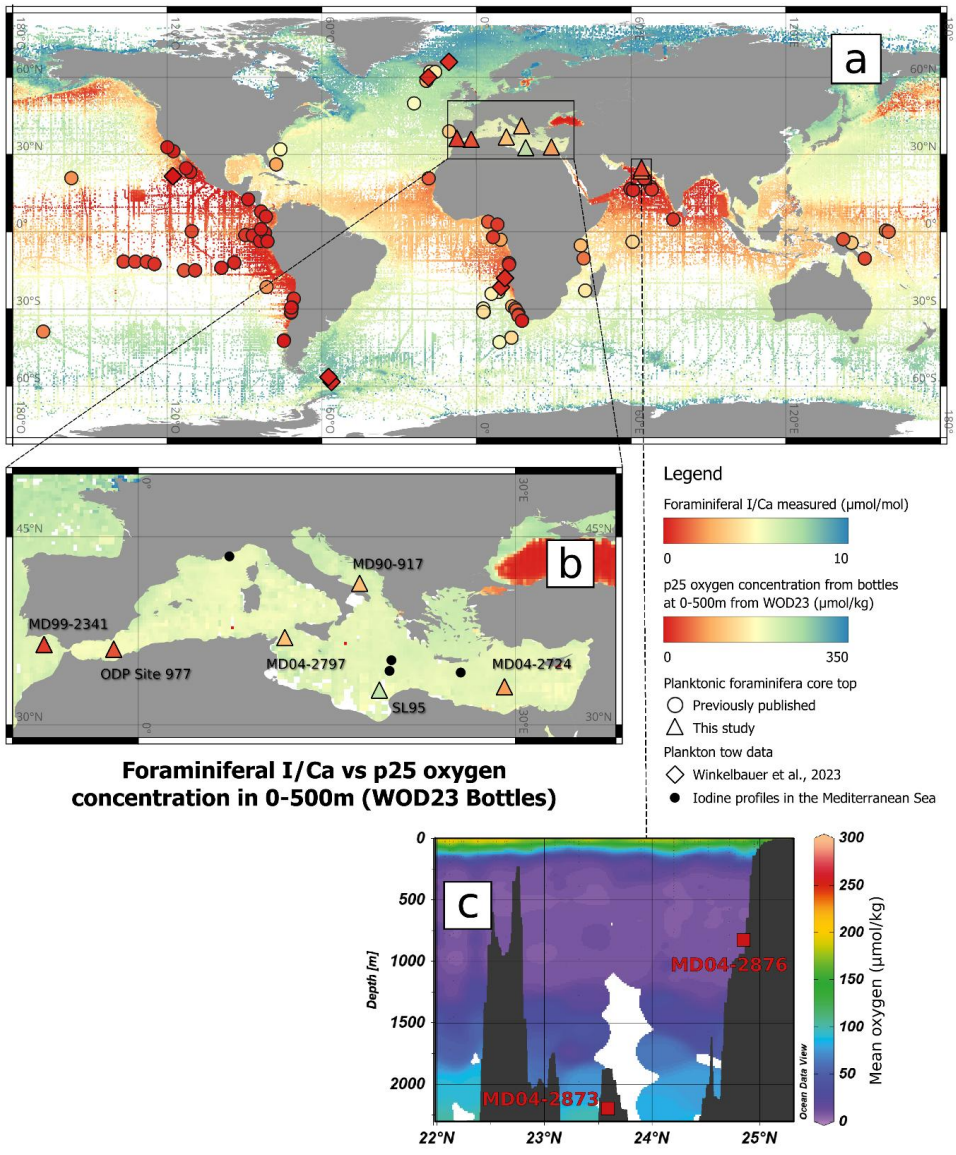


Figure 1: Map of 25th percentile of oxygen concentration (p25 [$O_2$]) in µmol/kg in ±0.25° (latitude and longitude) at 0–500 mbsl and symbols corresponding to modern foraminiferal I/Ca (µmol/mol) less than 8000 years (8 ka) before present (BP) at global scale (a) and in the Mediterranean Sea (b). The locations of new core top data from this study are represented with triangles and published values with circles. Plankton tow data from Winkelbauer et al. (2023) are represented with diamonds. Position of dissolved inorganic iodine species concentrations in the Mediterranean Sea are represented in black (Tian and Nicolas, 1995; Ullman et al., 1990). Oxygen distributions

https://doi.org/10.5194/egusphere-2026-622
Preprint. Discussion started: 12 February 2026


were obtained from World Ocean Database 2023 (WOD23) (Mishonov et al., 2024). Arabian Sea mean oxygen section (c) shows the position of the two core-top studied. MD04-2876 is in the core of the OMZ, and MD04-2873 is below. Oxygen profile is made with Ocean Data View (Schlitzer and Reiner, 2025).

### 1.2 Analysis of Iodine/Calcium ratio from planktonic foraminifera

For foraminiferal I/Ca analysis, 30 monospecific planktonic foraminiferal tests were picked from 250–355 µm fraction and cleaned following Barker et al. (2003) protocol. Depending on the core, different species are used. For Gulf of Cadiz, *Globigerinoides ruber albus* (hereafter referred to as *G. ruber*), *Globigerina bulloides*, *Trilobatus sacculifer* (without sack-like chamber), *Globigerinella siphonifera* and *Pulleniatina obliquiloculata* were picked. For the Alboran Sea, *G. ruber* and *G. bulloides* ratios were analysed. For MD04-2797, SL95, MD90-917 and the two cores from the Arabian Sea, only *G. ruber* was used. After cleaning, samples were dissolved with diluted nitric acid at 0.1 M (0.66%). The obtained solution was then centrifuged to separate any residual non-dissolved particles. After a calcium (Ca) concentration test to determine the necessary dilution factor for each sample, an aliquot for iodine measurement is stabilised with tetramethylammonium hydroxide (TMAH, SIGMA-ALDRICH) to obtain a 0.33% $HNO_3$-0.48% TMAH matrix. The solution is then diluted to a Ca concentration of 50 µg/mL (50 ppm). The remainder is diluted to obtain Ca concentration of 100 µg/mL to determine Ca, U, Mn, Fe and Al concentrations (Guarinos et al., in prep). In this study only I/Ca ratio is discussed. Elemental analysis is carried out using ICP-MS (Agilent 7500ce) at the CEREGE, France.

Table 1: Description of cores and planktonic foraminiferal species used for I/Ca analysis

| Core name | Location | Latitude | Longitude | Depth (mbsl) | Depth in core (cm) | Core top age (ka cal BP) | Species picked | Comment | Age model reference |
|---|---|---|---|---|---|---|---|---|---|
| MD99-2341 | Gulf of Cadiz | 36.383 | -7.533 | 577 | 2–4 | 1.02 | *G. ruber, G. bulloides, T. sacculifer, G. siphonifera, P. obliquiloculata* | Atlantic water inflow | Eynaud et al., 2009 |
| ODP Site 977 | Alboran Sea | 36.032 | -1.955 | 1984 | 23–25 | 1.37 | *G. ruber and G. bulloides* | Atlantic water inflow | Martrat et al., 2004 |
| MD04-2797 | Sicily Strait | 36.959 | 11.666 | 771 | 0–1 | 0.70 | *G. ruber* | Connection between basins | Cornuault et al., 2018 |
| SL95 | Gulf of Sirte | 32.774 | 19.191 | 1390 | 0–1 | 1.20 | *G. ruber* | South Ionian Sea | This study |
| MD04-2724 | Levantine Sea | 33.033 | 29.150 | 1659 | 5–6 | 6.00 | *G. ruber, T. sacculifer* | Deep Nile delta | This study |
| MD90-917 | Adriatic Sea | 41.280 | 17.620 | 1010 | 2–3 | 0.65 | *G. ruber* | Well oxygenated | Siani et al., 2010 |
| MD04-2873 | Pakistan Margin | 23.532 | 63.827 | 2196 | 1–2 | *NA* | *G. ruber* | Below the OMZ | Pichevin et al., 2007 |
| MD04-2876 | Pakistan Margin | 24.849 | 64.014 | 828 | 2–3 | *NA* | *G. ruber* | Within the OMZ | Bard et al., 2013 |

https://doi.org/10.5194/egusphere-2026-622
Preprint. Discussion started: 12 February 2026


Each sample is analysed and standard-sample bracketing is used to characterise instrumental drift during measurement. There is no currently certified geostandard for I/Ca but JCp-1, a coral powder, is commonly used in this role. In our analyses JCp-1 is measured every five samples. Our measure of I/Ca of JCp-1 is 4.34 ± 0.11 µmol/mol (n=27, 1sd). This is in good agreement with published values of 4.27 ± 0.10 µmol/mol (n=13, 1sd, Winkelbauer et al., 2023), 4.33 ± 0.06 µmol/mol (n=6, 1sd, Chai and Muramatsu, 2007), 4.27 ± 0.06 µmol/mol (1sd, Lu et al., 2010), and 4.20 ± 0.43 µmol/mol (1sd, Hess et al., 2025). Calculated I/Ca precision is better than 3% and blank levels were low, often below detection limits, so no correction is applied.

### 1.3 Inorganic iodine speciation depending on dissolved oxygen concentration

The concentration of inorganic iodine species in the ocean is primarily controlled by redox conditions, with iodate prevailing in oxic conditions and iodide dominating in reducing environments (Chance et al., 2014; Ullman et al., 1990). To establish the relationship between iodate and oxygen concentration, iodine data are expressed as iodate proportion in total inorganic iodine in order to avoid potential impacts from changing iodine concentration. Iodine speciation data from Bermuda inshore water are excluded (Jickells et al., 1988), as they originate from a highly restricted environment, and not representative of the conditions considered in this study. Data analysis is performed using least-squares fitting analysis in Python 3.12. The 95% prediction intervals are computed by propagating the uncertainties of the fitted model parameters contained in the covariance matrix. This combines both the variance of the fitted parameters and the residual variance of the data within the selected area.

To explore the influence of redox conditions on inorganic iodine speciation, oxygen data were combined with published iodine speciation measures. Inorganic iodine speciation in the upper 500 m is investigated using previously published data (Winkelbauer et al., 2023). Oxygen concentrations were obtained from World Ocean Database 2023 (WOD23) from Mishonov et al. 2024 from within a 0.25° area around each sampling site, where possible. From every obtained oxygen distribution, we determined the percentiles of oxygen concentration. Each measurement from 0–500 m at a given station is attributed to the same percentile value.

### 1.4 Planktonic foraminiferal I/Ca database

Planktonic foraminiferal I/Ca database is obtained with 15 new core top data (this study), and previously published core top and plankton tow measurements (Hess et al., 2025; Lu et al., 2020, 2016; Nilsson-Kerr et al., 2025; Winkelbauer et al., 2021, 2023; Zhou et al., 2022).

The database contains 567 core top data points, 438 of which are younger than 2,000 years BP. Oxygen distribution in the first 500 m are obtained from WOD23 accepted values (class 0) from i) Bottle (Winkler titration) and ii) Conductivity–Temperature–Depth (CTD) with oxygen sensor data in a 0.25° area around each sampling site (Mishonov et al., 2024). For sites where no oxygen profile is available, the area of search is extended to 0.5° and the data flagged, no data from >0.5° is used. The obtained oxygen concentration data are used to calculate the minimum, maximum, mean, and percentile values. CTD measurements are only used for 3 I/Ca values as they are considered to be less accurate because of excursion artifacts. For this reason, we prioritise bottle data which are consider to be more accurate.

https://doi.org/10.5194/egusphere-2026-622
Preprint. Discussion started: 12 February 2026


Additional environmental variables are included to assess their potential contribution to I/Ca variability. Other parameters, seawater temperature, salinity, nitrate, phosphate, chlorophyll, pH and alkalinity are similarly obtained from class 0 bottle measurements in 0.25° around sampling site at the first 500 m. Investigating the 0–500 m is crucial because this is where the planktonic I/Ca signal is presumed to originate (Lu et al., 2016). No value is attributed to sites without any available bottle measurement. Other parameters, net primary productivity (NPP) (Behrenfeld and Falkowski, 1997; Oregon State University ORCA, n.d.), current speed, and mixed layer depth, are obtained using their corresponding raster resolution. NPP is derived from annual mean satellite data integrated from 1998 to 2022 at a resolution of 25 km and using Eppley-Vertically Generalized Production Model (Eppley-VGPM). Parameters related to ocean dynamics are derived from Global Ocean Physics Reanalysis annual mean and maximum values ("Global Ocean Physics Reanalysis," 2025). We use absolute Northward and Eastward velocities from surface to 500 m and mixed layer depth. Data sources are listed in Table 2.

The database construction we propose here is a table format with two entries. Each line is a specific measure of foraminiferal I/Ca. Columns correspond to different characteristics of the measure, sampling site, and all the extracted site-specific parameters previously mentioned. Information of symbionts presence and habitat depth is also shown. The full database is available in supplementary material.

To assess the relationships between foraminiferal I/Ca and environmental variables, we use both Spearman's ρ and Kendall's τ correlation coefficients. Even if some individual uncertainties of the selected variables may follow normal distributions, the dataset as a whole is heterogeneous and non-normally distributed, making non-parametric tests more appropriate. Moreover, as the resulting relationships are likely non-linear, these rank-based methods provide a robust evaluation of correlation. The use of both correlation coefficients captures two complementary aspects of monotonic relationships: the strength of the association and how well the observations agree with each other. These analyses are intended to identify statistical covariation.

## 2 Results

### 2.1 Definition of p25 [$O_2$] and Iodine speciation

Oxygen concentration ranges from 0 to 300 µmol/kg. Obtained oxygen distribution in the upper 500 m layer at sites where foraminiferal I/Ca is available are mostly unimodal or multimodal (Fig. 2). Previous studies use the minimum [$O_2$] value measured in 0–500 m to calibrate foraminiferal I/Ca (Hess et al., 2025; Lu et al., 2020). The use of the minimum value can provide questionable representativeness of actual conditions because the minimum value could reflect exceptional events or data reporting issues. As the distribution of oxygen concentration at 0 to 500 m water depth is not normally distributed, we use the 25$^{th}$ percentile (p25) to represent average oxygen depletion instead of the minimum value. We have tested percentiles from 5 to 30 at each 5% (Fig. S1). All tested definition of X-axis shows the same slope, with only the intercept being different. We choose the higher $R^2$ (0.39) together with the lower Root Mean Square Error (RMSE) (1.356), corresponding to p25 (Fig. S1). We note here that p25 value is close to mean value minus 1 standard deviation when the distribution was normal or quasi-normal.

https://doi.org/10.5194/egusphere-2026-622
Preprint. Discussion started: 12 February 2026


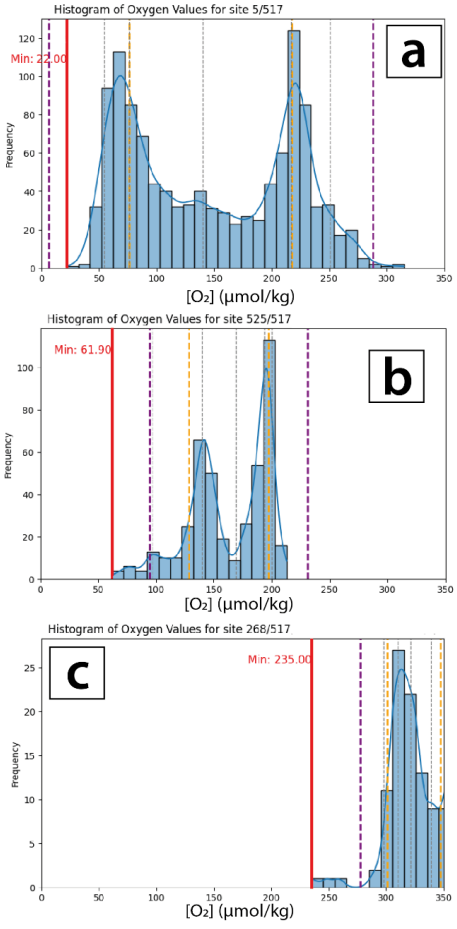


Figure 2: Histograms of common types of oxygen distributions encountered in this study, with OMZ-type from Mauritanian upwelling (a), intermediate from southwestern Pacific Ocean (b) and well oxygenated from North Atlantic (c) distributions. Oxygen depletion representative value p25 [$O_2$] is highlighted in full red line. Other percentiles are in dotted grey lines. Dotted red line is the minimum oxygen value previously used. Dotted yellow and purple lines are 1 sigma (68%) and 2 sigma (95%) limits, respectively. The difference between [$O_2$] min and p25 [$O_2$] is 0–142 µmol/kg. Note that the shown oxygen concentration range is different between (a), (b) and (c).

In strongly oxygen-depleted areas, such as OMZ, the oxygen distributions are mainly multimodal with high values near surface and lower values in the heart of OMZ (Fig. 2a). Those areas are represented with p25 [$O_2$] values ranging from 0 to 100 µmol/kg.

In areas with p25 [$O_2$] value between 100 and 180 µmol/kg (tropical Atlantic Ocean, Ontong Java Plateau in the tropical Pacific), the distribution of oxygen concentration is mostly multimodal, reflecting vertical change with water depth but with moderate oxygen depletion (Fig. 2b).

https://doi.org/10.5194/egusphere-2026-622
Preprint. Discussion started: 12 February 2026


Oxygenated waters are marked by p25 [$O_2$] values from 180 to 300 µmol/kg. The corresponding distributions are mostly unimodal (Fig. 2c). Some sites were not attributed to a distribution type due to their relative rarity.

### 2.2 Iodine speciation and oxygen concentration

Total inorganic iodine is in the range of 400 to 500 nM and is more or less constant in the ocean (Chance et al., 2010) (Fig. 3c). Inorganic iodine depletion near coastal regions have been attributed to biological uptake (Elderfield and Truesdale, 1980; Wong and Zhang, 1992). But inorganic iodine speciation primarily varies with redox potential, largely governed by oxygen availability (Luther, 2023). In order to compare inorganic iodine speciation to foraminiferal I/Ca, we represent it from the first 500 m as a function of p25 [$O_2$] in 0–500 m (Fig. 3a) and [$O_2$]min in 0–500 m. Speciation is shown as iodate/(iodate + iodide), that corresponds to the iodate proportion of the inorganic iodine concentration (Tian and Nicolas, 1995). This representation allows us to minimise the effect of inorganic iodine concentration (Elderfield and Truesdale, 1980; Tian and Nicolas, 1995).

Main result shows high dispersion of iodine speciation, and non-linear relationship (Fig. 3a and 3b). It also shows that iodate might exist in oxygen depleted waters, especially in Pacific Ocean. Iodine speciation is highly variable at 0–500 m. Iodate absence is mainly found at p25 [$O_2$] <10 µmol/kg although it is not systematically absent in those areas. In well oxygenated water (>200 µmol/kg), inorganic iodine is principally under the oxidised form, with a proportion above 60%. However, measurements from one site in Pacific and three in Atlantic are low in iodate proportions (<0.5) in oxygenated areas (>150 µmol/kg), and fall outside the prediction interval.

We choose an exponential fit function to represent the rapid iodate decrease when p25 [$O_2$] is below 20 µmol/kg and the plateau in oxygenated waters (p25 [$O_2$] >180 µmol/kg) (Fig. 3a). Prediction interval for exponential fit is represented in shaded red area. The objective of this representation is not to find the best fit, but rather to determine whether the relationship between iodate proportion and dissolved oxygen content could explain the variation in foraminiferal I/Ca-based oxygen reconstruction. Compared to [$O_2$]min (Fig. 3b), the use of p25 [$O_2$] (Fig. 3a) slightly improves the consistency of the relationship by limiting the influence of total inorganic iodine concentration change. The main difference in the x-axis definition is the change in range, from 0–280 µmol/kg for [$O_2$] min to 0–330 µmol/kg for p25 [$O_2$] (Fig. 3a, b). This results in a visually stretched dataset in the x-direction but does not affect the dispersion along the y-axis. Moreover, fewer values fall outside the 95% prediction interval in the high-iodate-proportion / low-p25 range compared to [$O_2$] min. A few points fall below the 95% prediction interval at intermediate oxygen levels when using p25 [$O_2$].

https://doi.org/10.5194/egusphere-2026-622
Preprint. Discussion started: 12 February 2026


In the Mediterranean Sea, inorganic iodine speciation profiles are scarce, with only one time series and four different locations reported (Tian and Nicolas, 1995; Ullman et al., 1990). Nevertheless, consistently high iodate concentrations are observed in the upper 0–500 m (370–515 nmol/L) corresponding to well oxygenated water ([$O_2$]min 100–180 µmol/kg) (Fig. 3b). Under these conditions, iodate represents more than 80% of total inorganic iodine, with p25 [$O_2$] between 190 and 200 µmol/kg.

Figure 3: Iodate proportion in total inorganic iodine, iodate/(iodate+iodide) in 0–500 m as a function of p25 (a) (Spearman ρ = 0.625, Kendall τ = 0.447, p-values <0.01) and iodate concentration as a function of minimum (b)

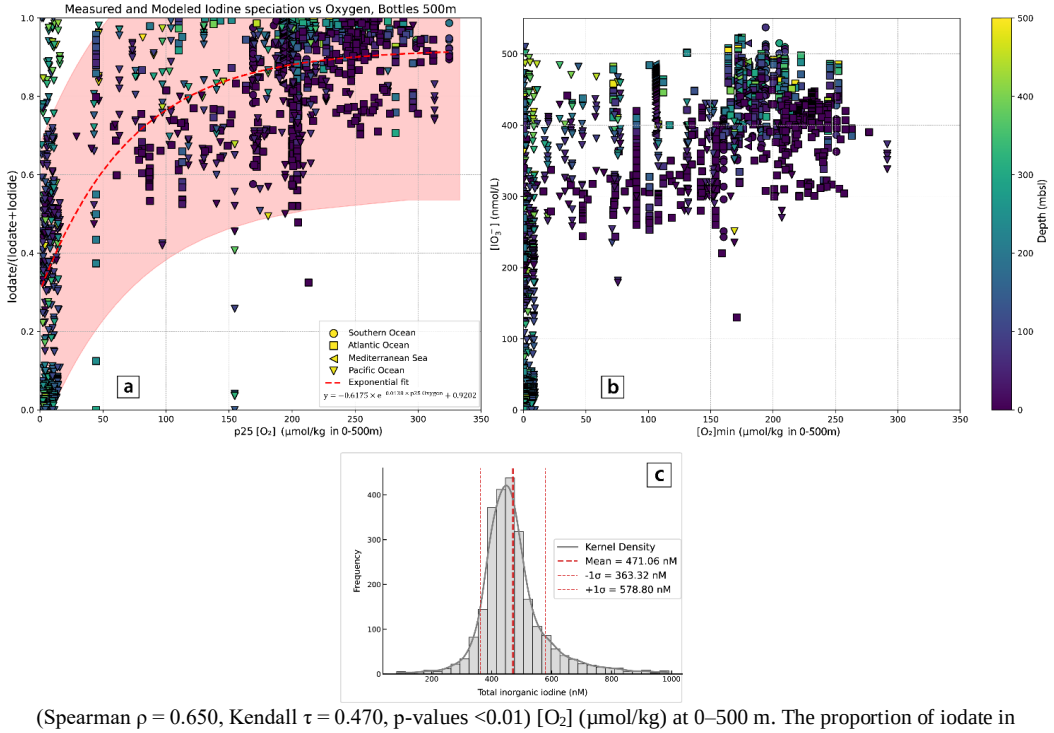


(Spearman ρ = 0.650, Kendall τ = 0.470, p-values <0.01) [$O_2$] (µmol/kg) at 0–500 m. The proportion of iodate in inorganic iodine was obtained from Winkelbauer et al. (2023) and are classified by ocean. Red dotted line is the exponential fit of this relation (y = -0.6175*exp(-0.0138*x) + 0.9202 for p25), with the 95% prediction interval filled in red. Total inorganic iodine distribution with mean and ±1σ values (c).

### 2.3 New core top planktonic foraminiferal I/Ca

Low iodine concentration in foraminifera, ranging from 0 to 2 µmol/mol, are mostly found with p25 [$O_2$] between 0 and 180 µmol/kg (Fig. 4) In the 180–300 µmol/kg of p25 [$O_2$], most foraminiferal I/Ca ratios show higher values ranging from 1 to 8 µmol/kg.

https://doi.org/10.5194/egusphere-2026-622
Preprint. Discussion started: 12 February 2026


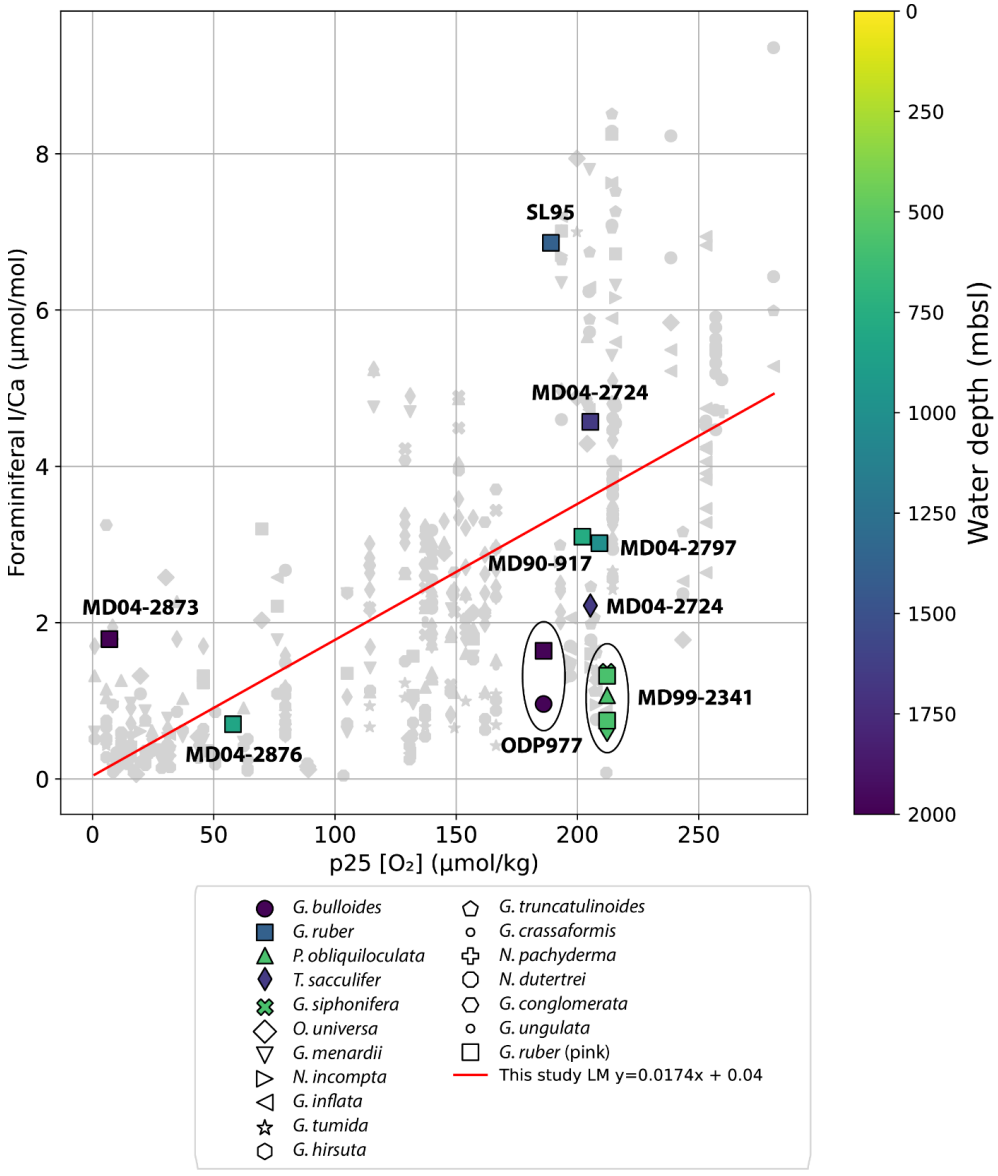


Figure 4: Core top foraminiferal I/Ca (µmol/mol) as a function of p25 [$O_2$] concentration (µmol/kg) for samples more recent than 8 ka BP. New measures (n=15) from this study are coloured as water depth (mbsl) and identified with colour code. Previously published values are represented in grey. All foraminiferal species are differentiated by symbols. Red linear regression was obtained using all data <2 ka BP.

New core top data from the Pakistan margin present I/Ca values lower than 2.5 µmol/mol (0.7 µmol/mol for MD04-2876 and 1.8 µmol/mol for MD04-2873). Difference in p25 [$O_2$] could be related to oxygen data availability with wider area of oxygen distribution of 0.5° for MD04-2873 instead of 0.25° for MD04-2876 and different number of oxygen profiles (n=2 and n=7 respectively).

https://doi.org/10.5194/egusphere-2026-622
Preprint. Discussion started: 12 February 2026


In the Mediterranean Sea, foraminiferal I/Ca values are very low in highly oxygenated areas (1.0 µmol/mol in the Gulf of Cadiz and 1.6 to 3.1 µmol/mol in Alboran Sea) that corresponds to p25 [$O_2$] between 180 and 220 µmol/kg (Fig. 4). The observed trend cannot be explained by vertical oxygen structure or by seasonal oxygen-depletion events, as dissolved oxygen profiles in the upper 500 m show very limited seasonal or inter-annual variability, even when more than 20 profiles per site are considered. Regarding I/Ca difference between planktonic foraminiferal species, three cores provide information (Table 1). The dispersion of different species of foraminifera is around 40% for the Gulf of Cadiz (MD99-2341) and the Alboran Sea (ODP Site 977) whereas in the Eastern Mediterranean Sea the high I/Ca ratios (from 2 to 6 µmol/mol) are associated with a dispersion of 50% for the deep Nile Delta core (MD04-2724).

Iodine incorporation during particle sinking has been proposed to explain the low I/Ca values from plankton tows (Winkelbauer et al., 2023). However, we find no systematic relation with water depth and I/Ca with our new data (Fig. 4). Deep sites in oxygenated water like ODP Site 977 at 1984 mbsl also show very low I/Ca. Other cores at comparable depths and oxygenation levels, like MD04-2724 at 1659 mbsl show I/Ca above 4 µmol/mol.

### 2.4 Planktonic I/Ca values and the environmental parameters on global scale

The relationship between environmental parameters such as biogeochemical characterisation of 0–500 m at each site, primary productivity and physical parameters (current velocity) and foraminiferal I/Ca is investigated using statistical test Kendall's τ and Spearman's ρ correlation coefficients (Table 2). We only include samples more recent than 2 ka BP in the statistical analysis because older samples are less likely to be representative of modern conditions. The results are reported in Table 2.

Table 2: Results of statistical correlation test for environmental variables and planktonic foraminiferal I/Ca for samples more recent than 2 ka BP. Tested parameters are listed from highest to lowest absolute Spearman's ρ.

| Variable | n | Spearman ρ | Spearman p-value | Kendall τ | Kendall p-value | Data source |
|---|---|---|---|---|---|---|
| Maximum 500m depth MLD* | 446 | 0.69 | <0.01 | 0.5 | <0.01 | CMEMS GLORYS12V1 |
| Minimum Oxygen* | 421 | 0.67 | <0.01 | 0.45 | <0.01 | WOD23 |
| Mean Oxygen (all depths)* | 419 | 0.67 | <0.01 | 0.47 | <0.01 | WOD23 |
| Mean Oxygen* | 421 | 0.65 | <0.01 | 0.47 | <0.01 | WOD23 |
| p25 Oxygen* | 421 | 0.65 | <0.01 | 0.46 | <0.01 | WOD23 |
| Mean 500m depth MLD* | 446 | 0.63 | <0.01 | 0.43 | <0.01 | CMEMS GLORYS12V1 |
| Bottom mean Oxygen* | 442 | 0.62 | <0.01 | 0.44 | <0.01 | WOD23 |
| Minimum pH* | 110 | 0.46 | <0.01 | 0.29 | <0.01 | WOD23 |
| Mean Phosphate* | 277 | -0.45 | <0.01 | -0.32 | <0.01 | WOD23 |
| Maximum Chlorophyll depth* | 182 | -0.34 | <0.01 | -0.23 | <0.01 | WOD23 |
| Net Primary Productivity VGPM* | 441 | -0.3 | <0.01 | -0.2 | <0.01 | Orca Ocean Productivity |
| Maximum Oxygen* | 421 | 0.28 | <0.01 | 0.19 | <0.01 | WOD23 |
| Age (ka BP) | 78 | -0.26 | 0.074 | -0.19 | 0.059 | See database |
| Distance to coast (km)* | 444 | 0.25 | <0.01 | 0.17 | <0.01 | Calculated |
| Mean Temperature* | 404 | -0.25 | <0.01 | -0.15 | <0.01 | WOD23 |

https://doi.org/10.5194/egusphere-2026-622
Preprint. Discussion started: 12 February 2026


| | | | | | | |
|---|---|---|---|---|---|---|
| Mean pH | 110 | 0.18 | 0.121 | 0.15 | 0.074 | WOD23 |
| Latitude* | 446 | -0.15 | <0.01 | -0.09 | 0.027 | See database |
| Maximum 500m depth velocity* | 446 | 0.15 | <0.01 | 0.09 | 0.015 | CMEMS GLORYS12V1 |
| Mean Alkalinity | 74 | 0.14 | 0.37 | 0.11 | 0.328 | WOD23 |
| Mean Salinity* | 404 | 0.13 | 0.028 | 0.1 | 0.019 | WOD23 |
| Maximum Chlorophyll | 182 | 0.1 | 0.261 | 0.05 | 0.44 | WOD23 |
| Water depth (m) | 446 | 0.05 | 0.4 | 0.01 | 0.75 | See database |
| Mean Nitrate | 251 | -0.05 | 0.547 | -0.03 | 0.618 | WOD23 |
| Mean 500m depth velocity | 446 | -0.02 | 0.715 | -0.02 | 0.664 | CMEMS GLORYS12V1 |
| Depth in core (cm) | 406 | -0.01 | 0.84 | -0.01 | 0.818 | See database |

*: statistically significant correlations

All oxygen related variables (minimum, maximum, mean, p25, mean (all depths) and bottom mean oxygen) are significantly linked to foraminiferal I/Ca with coefficients above 0.6 and 0.4 for Spearman's ρ and Kendall's τ, respectively, and p-values less than 0.01 for both cases (Table 2). Maximum mixed layer depth shows the highest correlation coefficients, but this parameter is also tightly linked to oxygen (Fig. S2). This observation supports an oxygen control on foraminiferal I/Ca, although the quantitative relationship remains uncertain.

Minimum pH, phosphate and maximum chlorophyll depth present correlation with I/Ca (Table 2) but they also covary with p25 [$O_2$] and are thus not independent (Fig. S2). Distance to coast, mean temperature, latitude, maximum current velocity, and mean salinity also show significant correlations with foraminiferal I/Ca. However, their correlation coefficients are less than half those of the strongest correlations identified. These variables are therefore not further discussed as primary drivers of foraminiferal I/Ca variability.

Depth in core and sediment age are examined to evaluate a potential early diagenesis effect. Most of the core top selected for this study are sampled close to the water-sediment interface and in various environments. Those two variables do not show any statistically significant correlation with foraminiferal I/Ca on global scale. This is equally true with water depth above the core sites as already examined with the new data (Fig. 4), no clear correlation is visible.

### 2.5 Multi-species foraminiferal I/Ca and calcification depths on global scale

Symbiont presence in foraminifera could also alter the incorporation of specific elements like anions because of so-called "vital effects" (Hönisch et al., 2003). We have classified the symbiosis behaviour of the species and represent their I/Ca as a function of p25 [$O_2$] (Fig. S3), we note the absence of specific patterns. No group is enriched or depleted in iodine compared to the others. The slopes for linear regression are very close (0.016 or 0.017). Symbiont barren species are found in all defined domains, but the low I/Ca plankton tow with p25 [$O_2$] concentration >250 µmol/kg are exclusively symbiont barren species.

In the database, we have also classified species in three zones of calcification depths as the local concentration of iodate changes with depth and influences foraminiferal I/Ca (Hess et al., 2025). Species are classified as surface, shallow subsurface, and deep subsurface dwellers following Hess et al. (2025). Figure S4 presents the linear fit of the I/Ca ratios and p25 [$O_2$], which is obtained by classifying foraminifera according to their calcification depth.

https://doi.org/10.5194/egusphere-2026-622
Preprint. Discussion started: 12 February 2026


The main result is a similar slope for the three groups (0.015 to 0.019). Differences in intercepts are not interpreted due to the important impact of scattering.

## 3 Discussion

A gain in iodine in foraminiferal test during their post-mortem settling to the seafloor was proposed to explain low plankton tow values (Winkelbauer et al., 2023). This implies an increase in I/Ca with water depth. However, water depth does not show any significant covariation with foraminiferal I/Ca (Table 2 and Fig. S5). We thus consider that the influence of iodine accumulation during the foraminifera settling would be secondary and could be hidden under a stronger oxygen control. No specific pattern for foraminiferal I/Ca as a function of oxygen can be highlighted by using foraminiferal species, calcification depth groups, or symbiont presence/absence.

In the following, we will at first discuss the possible reasons for a larger scatter observed between iodate proportion and p25 [$O_2$] (Fig. 3). Then, a new calibration of foraminiferal I/Ca ratios against p25 [$O_2$] will be proposed (Fig. 5). The influence of the scattered relationship between iodate proportion and p25 [$O_2$] on the calibration will be evaluated (Fig. 6). Then, we will quantify residuals that are not supported by oxygenation changes to identify parameters affecting foraminiferal I/Ca (Table S1). A comparison between foraminiferal I/Ca and the value of synthetic calcite will provide us possible impact of vital effects (Fig. 6). Finally, we will examine the contribution of authigenic calcite to the Mediterranean samples (Fig. 7) that are characterised by low I/Ca ratios under oxic condition (Fig. 4).

### 3.1 Principal role of oxygen and possible reasons for a larger scatter observed between iodate proportion and p25 [$O_2$]

First order results suggest clear covariation of foraminiferal I/Ca with oxygen and oxygen related variables (Table 2). Oxygen variables show a positive trend with foraminiferal I/Ca. This covariation ranges from linear to exponential, and displays substantial scatter. Other parameters exhibit no consistent relationship, except oxygen-linked variables such as nutrients, NPP, and mixed-layer depth (Table 2 and Fig. S2).

Inorganic iodine speciation is theoretically controlled by redox potential, largely governed by oxygen availability (Luther, 2023). In practice, however, field observations frequently deviate from this thermodynamic framework (Fig. 3). The relationship between iodate and p25 [$O_2$] is strongly non-linear and exhibits important scatter. The dispersion likely reflects spatial and temporal variability in iodine redox cycling across regions and seasons. This mismatch between oxygen and iodate concentration may at least partly explain the apparent presence of iodate in waters here defined as oxygen-depleted.

As iodine speciation is sensitive to short-term oxygen fluctuations and depth-specific redox structure, this statistical approach better represents the oxygen conditions than relying on the minimum value. The observed scatter likely reflects a combination of true environmental heterogeneity and the limitations of matching discrete iodine measurements with oxygen data. The iodate–oxygen relationship in Fig. 3 shows that iodate proportion does not decline uniformly with decreasing oxygen. Consequently, at low p25 [$O_2$], the variability in the proportion of iodate can generate substantial scatter in foraminiferal I/Ca, potentially producing a factor of ~5 spread (1.0–

https://doi.org/10.5194/egusphere-2026-622
Preprint. Discussion started: 12 February 2026


5.0 µmol/mol) near 50 µmol/kg. Therefore, uncertainty in inorganic iodine speciation, both estimation errors or natural variability, remains a major source of scatter in the I/Ca–oxygen relationship.

### 3.2 A new calibration of planktonic foraminiferal I/Ca using p25 [$O_2$]

In our calibration, we use foraminiferal I/Ca as a function of p25 [$O_2$] concentration in 0–500 m, a representative value for oxygen concentration at each sampling site.

Figure 5 shows core top samples more recent than 2 ka BP considering possible temporal changes in dissolved oxygen concentration in the ocean. The linear fit shown in red in Fig. 5 corresponds to a Least Absolute Deviations (LAD) regression. This method was selected because it is more robust to outliers and large deviations than ordinary least squares. Its reliance on medians rather than means makes it particularly suitable when the error structure is non-Gaussian or affected by outliers.

The obtained new calibration equation is as follows:

$$Planktonic\ foraminiferal\ I/Ca\ (\mu mol/mol) = 0.0174 * p25\ [O_2]\ (\mu mol/kg) + 0.04 \quad (1)$$

Equation 1 provides a slightly better fit regarding precedent calibration from Hess et al. (2025) as shown by RMSE (Fig. 5a, b). This comparison integrates the recent results published by Nilsson-Kerr et al. (2025). The main difference between the two calibrations is that the clustered point at near-zero oxygen has been expanded in our case, covering a wider range of oxygen concentrations. Also, the intercept is lower, approaching I/Ca = 0 µmol/mol in strongly oxygen depleted waters (p25 [$O_2$] <10 µmol/kg). The points with low I/Ca (<2 µmol/mol) in oxygenated water correspond to samples from the Mediterranean Sea (this study) and one from Southern Benguela (Lu et al., 2020).

In order to identify secondary parameters that may influence foraminiferal I/Ca, the residuals are calculated using equation (1). The residuals are then plotted against multiple ocean variables (Fig. S6). Table S1 summarises the correlation coefficients and significance of the parameters tested. No clear nor visible trend can be highlighted within the global dataset including water depth or distance to coast.

https://doi.org/10.5194/egusphere-2026-622
Preprint. Discussion started: 12 February 2026


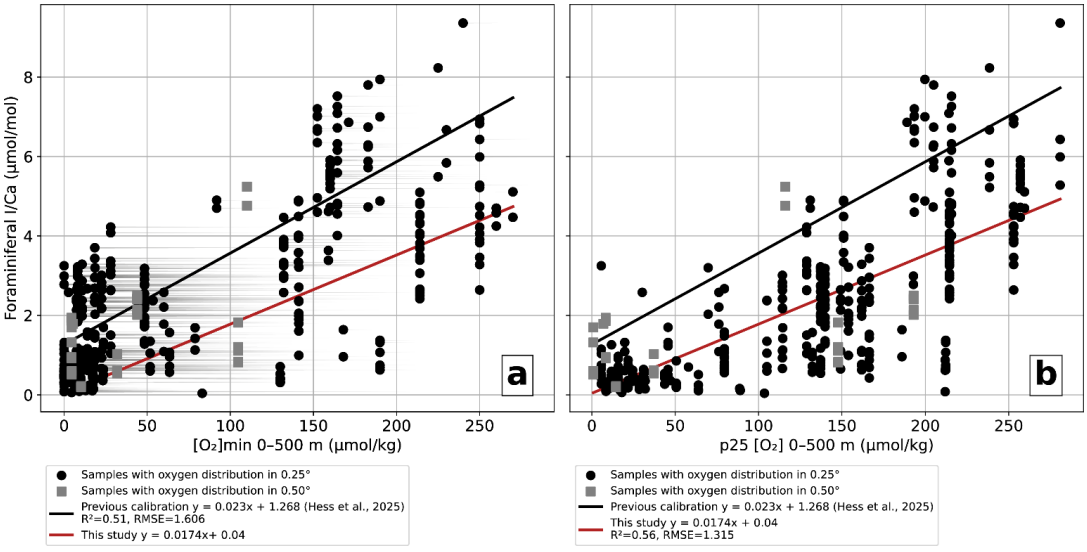


Figure 5: Foraminiferal I/Ca <2 ka BP as a function of minimum (a) and p25 (b) [$O_2$] in 0–500m. The same dataset is used for the two figures. Only the X-axis definition is different. Black line is the linear model calibration curve from (Hess et al., 2025). The red line is the linear model proposed in this study. Samples with oxygen distribution from 0.25° area are represented as black circles, and from 0.5° as grey squares. Horizontal lines in (a) illustrate the effect of X-axis change on dataset, highlighting that many low [$O_2$]min sites are shifted to higher representative oxygen depletion p25[$O_2$]. This is especially true for [$O_2$]min <50 µmol/kg and I/Ca >2 µmol/mol. No specific pattern emerges within the wider area.

### 3.3 A comparison of the I/Ca ratio of foraminifera with the value of synthetic calcite.

We further compare the new calibration with the relationship proposed for synthetic calcite (Zhou et al., 2014). The experience of synthetic calcite precipitation in iodate-rich medium indicated a linear relationship between calcite I/Ca and iodate concentration (Lu et al., 2010; Zhou et al., 2014). For the comparison, the iodate concentration in the medium is converted to oxygen concentration using the relationship between iodate proportion and p25 [$O_2$] concentration (Fig. 3a). Total inorganic iodine concentration is considered to be 471 nM (Fig. 3c) and calcite is assumed to be precipitated at 19°C.

In Figure 6, the synthetic calcite I/Ca relationship is shown in blue, with the 95% prediction interval (blue shaded area). The 95% prediction interval is large, implying a large potential impact on our calibration. This indicates that iodate concentration relative to oxygen plays a key role in generating the observed dispersion in foraminiferal I/Ca. The abiotic incorporation of iodine is of the same order of magnitude as that found in foraminifera. Iodine incorporation into carbonates likely reflects predominantly abiotic processes. However, some foraminifera I/Ca ratio falls out of the prediction interval. Below 200 µmol/kg $O_2$, most I/Ca values are below the values that can be explained by abiotic calcite precipitation, until severe oxygen depletion (<20 µmol/kg) where foraminifera I/Ca return to the abiotic level. The highest foraminiferal I/Ca values (>6 µmol/mol) are in the highly oxygenated area (>180 µmol/kg) and are above the abiotic interval (Fig. 6). Those observations suggest the presence of unknown parameters that are specific for foraminiferal calcite (e.g. microenvironment, changes to growth rate…). Zhou et

https://doi.org/10.5194/egusphere-2026-622
Preprint. Discussion started: 12 February 2026


al. (2014) showed the temperature dependency of partition coefficient (Kd) of iodine for abiotic calcite. But no systemic behaviour could be highlighted explaining higher or lower foraminiferal I/Ca anomalies with temperature differences (Fig. 6).

To summarise, inorganic iodine speciation has a non-linear relationship with dissolved oxygen concentration although the observed pattern for foraminiferal I/Ca does not follow the exponential trend that is expected from the relationship between iodate proportion and p25 [$O_2$] (Fig. 6). Low I/Ca values found in oxygenated area might be caused by reduced iodine incorporation, related to unknown mechanisms/conditions. Since no mechanism has yet been identified to justify a specific fitting curve for I/Ca ratio, we consider that the linear regression is an appropriate approximation. The dispersion of I/Ca values might be caused by the relationship between iodine speciation and oxygen concentration that could account for ~75% of the variance compatible with the model's 95% prediction interval (assuming constant total inorganic iodine), and up to ~93% by considering ±1σ uncertainty in total inorganic iodine from Fig. 4b (Fig. S7). This dispersion likely represents the second key explaination for I/Ca values in foraminifera. However, it remains that low I/Ca in highly oxygenated water seems to be related to an incorporation mechanism that remains unknown, given its systematic offset from the predicted values. This offset is potentially related to vital effects discriminating iodine incorporation, or to iodine speciation.

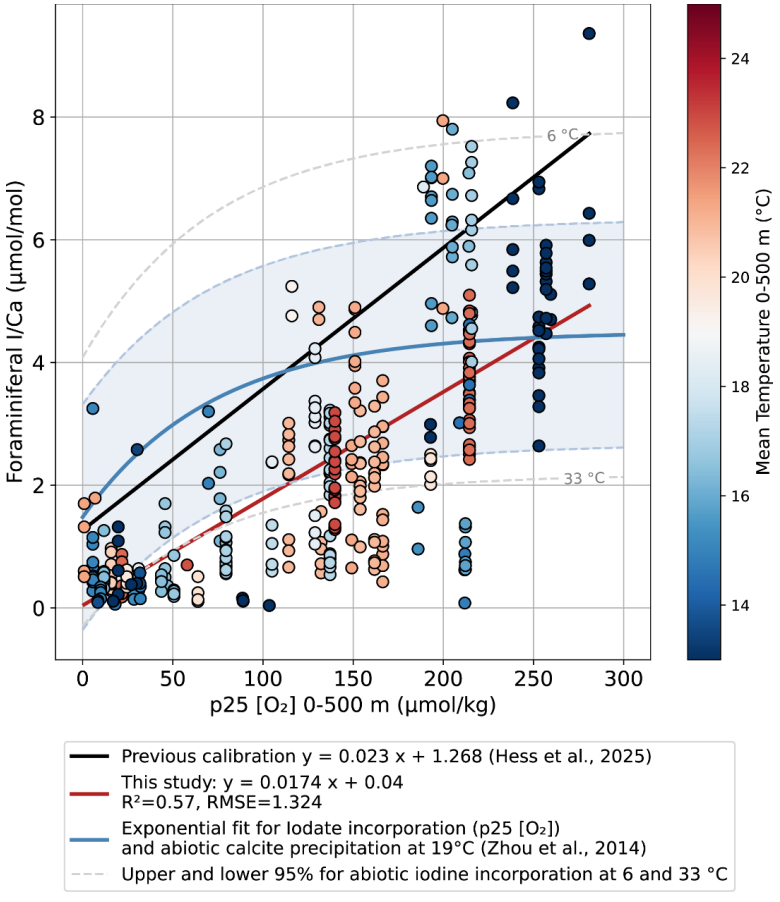

https://doi.org/10.5194/egusphere-2026-622
Preprint. Discussion started: 12 February 2026


Figure 6: Foraminiferal I/Ca <2 ka BP as a function of p25 [$O_2$] in 0–500 m. The red line is the linear model proposed in this study. Blue curve represents the abiotic incorporation of iodine following iodate proportion in total inorganic iodine determined in Figure 3 and assuming a mean concentration of total inorganic iodine of 471 nM (Fig. 3c). The abiotic incorporation was determined following (Zhou et al., 2014). Blue area corresponds to 95% prediction interval also determined in Figure 4 for a temperature of 19 °C. 57% of the data fall in this prediction interval. Temperature from 6 to 33 °C are considered for the maximum and minimum 95% prediction interval (grey dashed lines).

### 3.4 Authigenic contribution via secondary calcite precipitation

Depth in core and age were not significantly correlated with foraminiferal I/Ca based on first-order statistical tests (Table 2). However, these parameters do not fully capture the potential influence of diagenesis or secondary calcite precipitation, which may be particularly important within the sediments from OMZ and the Mediterranean Sea which are characterised by high alkalinity pore/bottom waters. This section therefore examines whether early diagenetic carbonate precipitation could contribute to the observed variability in I/Ca.

Because authigenic carbonates typically have very low I/Ca (Lu et al., 2010), the lower I/Ca value of MD04-2876 (Arabian Sea, OMZ core) relative to MD04-2873 (below the OMZ) could partly reflect the presence of authigenic carbonates formed under reducing conditions. In the marine sediments of the OMZ, the increase in alkalinity of the pore water due to anaerobic respiration leads to the precipitation of authigenic carbonates (Suess, 1979; Meister et al., 2022). In the Mediterranean Sea, high water-column alkalinity driven by excess evaporation (Schneider et al., 2007) promotes authigenic carbonate precipitation, as shown by high Mg/Ca ratios in foraminifera (Boussetta et al., 2011).

Figure 6 presents p25 [$O_2$] alongside the expected foraminiferal I/Ca predicted from Equation (1) with a black line. Sensitivity tests were performed using a binary mixing model between the expected foraminiferal I/Ca and authigenic carbonates assuming an I/Ca of 0.06 µmol/mol for authigenic carbonate (Lu et al., 2010). For the Arabian Sea OMZ core, measured I/Ca values fall below the expected ratio and could correspond to a 30–40% mass contribution of low I/Ca secondary carbonate. In contrast, MD04-2873 (below the OMZ) displays higher I/Ca than expected, likely due to poorly constrained oxygen variability resulting from the limited number of available oxygen profiles (section 3.2).

In the Mediterranean Sea, the two eastern basin cores (SL95 and MD04-2724) show I/Ca values above expectation, while others fall below. Cores MD04-2797 and MD90-917 are slightly depleted in I/Ca relative to the value estimated from equation (1) and could reflect a 10–20% contribution of authigenic carbonates. However, the samples from the western basin (ODP Site 977) and from the Gulf of Cadiz (MD99-2341) would require an implausibly high 60–90% contribution of authigenic calcite to explain their (much-)lower-than-expected I/Ca. Such a contribution is unrealistic, as authigenic calcite precipitation is far less common in the western basin, and extensive overgrowths would have been excluded (Crudeli et al., 2004).

Overall, secondary calcite precipitation cannot fully explain the lower I/Ca deviations. Low I/Ca values occur in regions where early diagenetic calcite formation is low, while no mechanism has been identified to account for

https://doi.org/10.5194/egusphere-2026-622
Preprint. Discussion started: 12 February 2026


I/Ca values higher than expected, nor for the scatter observed among species dwelling at the same depth within the same core top samples, except for as yet undefined vital effects.

We conclude that foraminiferal I/Ca primarily reflects local oxygen variability through its control on iodine speciation. The Mediterranean Sea samples exhibit a similar behaviour and degree of scatter as those from other ocean basins, indicating that the proxy remains applicable in this semi-enclosed environment. However, the use of the proxy must focus on relative variability combined with another independent approach. The relationship between foraminiferal I/Ca and oxygen concentration may be site-specific, because it could be influenced by local environmental characteristics or processes that are not yet fully understood. This limitation is particularly relevant for coastal sites, including those within the Mediterranean Sea, where additional factors may modulate iodine speciation or iodine incorporation.

While foraminiferal I/Ca provides a semi-quantitative estimation of local oxygenation conditions, the core top values observed in the western Mediterranean Sea is as low as the values of plankton tow. This calls for caution when using this proxy alone for quantitative reconstructions.

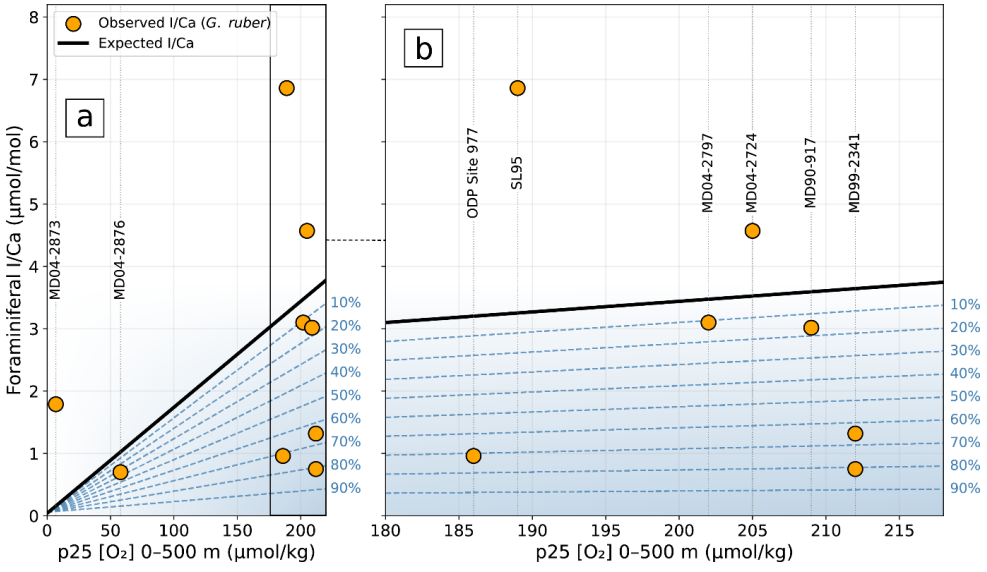


Figure 7: Foraminiferal I/Ca from the Mediterranean and Arabian Sea as a function of p25 [$O_2$] 0-500 m in whole p25 [$O_2$] range (a) and for p25 [$O_2$] >180 µmol/kg (b). Expected foraminiferal I/Ca from LAD from figure 5 is represented as black line. Grey dotted lines indicates deviation from expected value by increasing authigenic carbonate contribution from 10 to 90 %. Authigenic carbonate I/Ca was fixed at 0.06 µmol/mol following Lu et al. (2010).

### 3.5 Other possible factors

Oceanographic variables investigated other than oxygen did not show strong relationship with foraminiferal I/Ca (Table 2). Other parameters may also influence iodine speciation but were not highlighted through the statistical

https://doi.org/10.5194/egusphere-2026-622
Preprint. Discussion started: 12 February 2026


analysis conducted on foraminiferal I/Ca in this study. Previous works have shown that iodine speciation varies with distance to the coast, with iodate depletion toward productive coastal water (Wong and Zhang, 1992). The effect of distance to coast is absent on global scale, but it could be important at regional scale, such as in the Mediterranean Sea. This depletion is thought to be driven by enhanced biological iodine uptake through primary productivity. Although the Mediterranean Sea is highly oligotrophic, coastal and shelf regions can sustain episodes of high primary productivity (Packard et al., 1988; Powley et al., 2017), which could potentially influence iodate concentration. Only limited inorganic iodine vertical profiles (iodate and iodide) exists in the Mediterranean Sea (Fig. 1b), with one time series in the north western basin (Tian and Nicolas, 1995). The study showed limited variability across the year with iodate concentrations of 410–480 nM, but iodine speciation was measured in different oceanographic settings as the investigated locations in this study. So, different inorganic iodine behaviours may occur. Moreover, the variability of iodate concentration observed in the north western Mediterranean Sea, about 10%, does not explain the scattering in I/Ca observed.

Part of the variability may also not be fully constrained with the statistical analysis conducted (Tables 2 and S1, Figures S2 and S5). In fact, we conducted the analysis on the global dataset, with every site being a unique context and oceanographic settings. If we highlighted the first and most important role of oxygen as an I/Ca control, secondary parameters may not be fully captured. Inorganic iodine speciation remains poorly understood. Also, the influence of growth rate (calcification kinetics) could not be ruled out, and was never tested for I/Ca ratio (e.g. Allen et al., 2016). This has not been demonstrated but competition with other anions remains plausible as coupled substitution is required for the incorporation of $IO_3^-$ into $CaCO_3$ (Ram and Erez, 2023).

For future work, foraminifera culture with isolation of single parameters/monitoring of multiple parameters could help better constrain the proxy behaviour, alongside field studies. In particular, plankton tow observations showing systematically low foraminiferal I/Ca values suggest that limited incorporation at surface may happen, leaving open the question of when and where iodine is incorporated. Inorganic iodine speciation is still poorly constrained and further research is needed to understand its dynamics and incorporation in calcite lattice. Iodine incorporation sites, inside the structure of the shell or outside, as secondary precipitation, is hardly needed to distinguish iodine provenance in the foraminiferal test.

## Conclusions

In this study, we investigate planktonic foraminiferal I/Ca as a proxy for subsurface oxygen changes by integrating multiple environmental parameters. We first proposed a new definition of a representative oxygen depletion value in subsurface waters, accounting for local oxygen variability. Local oxygen distributions were unimodal or multimodal, reflecting both seasonal and depth-related oxygen variation. Planktonic foraminiferal I/Ca from core top samples showed a positive correlation with this representative minimum oxygen value, p25 [$O_2$], supporting the dominant control of oxygen on iodine presence and reinforcing the utility of the proxy to reconstruct past oxygenation changes.

https://doi.org/10.5194/egusphere-2026-622
Preprint. Discussion started: 12 February 2026


Despite this relationship, substantial amount of data dispersion remains. We explored several potential sources of scatter and found that the largest contribution likely arises from variability in inorganic iodine speciation. The global relationship between iodate and p25 [$O_2$] alone could account for more than 85% of the observed scatter.

No first-order relationship was found between water depth and foraminiferal I/Ca. This observation implies that iodine gain during particle sinking (Winkelbauer et al., 2023) could not be confirmed.

We propose a new calibration for subsurface oxygen depletion reconstruction based on planktonic foraminiferal I/Ca. By using p25 [$O_2$] values, we reduce the dispersion observed in previous calibrations. To maintain simplicity for paleo-applications, core top data younger than 2 ka BP were included regardless of species. Remaining dispersion may result from vital or species-specific effect, or other uninvestigated parameters, such as inorganic iodine speciation, which is difficult to constrain.

Finally, secondary calcite contribution was considered as a potential contributor to the low foraminiferal I/Ca values, given that secondary calcite formed in high alkalinity environment could dilute the signal. However, such an effect would require more than 60% of secondary calcite to explain western Mediterranean Sea values, which is implausible.

We therefore support the use of planktonic foraminiferal I/Ca as a semi-quantitative proxy for oxygenation state, consistent with Hess et al. (2025). This proxy can be applied to semi-enclosed basins to reconstruct relative variability when complemented with another independent approach.

## Appendices

## Data availability

Data supporting this paper will be available in the following repository: https://doi.org/10.5281/zenodo.18390413

The data is under review, the DOI is not activated yet.

## Author contribution

KT and VG designed the study; KT, MG and VG performed the laboratory procedures; VG have conducted the statistical analysis. VG wrote the manuscript with contributions from all authors.

## Competing interests

The authors declare that they have no known competing financial interests or personal relationships that could have appeared to influence the work reported in this paper.

## Acknowledgements

This work is supported by the French national project ANR MedSens (ANR-19-CE01-0019) granted to KT. Radiocarbon dating was performed at the LMC14 laboratory as a part of the French ARTEMIS program. Sample preparation and analytical measurements were supported by the LPM platform (Sandrine Conrod), the LGO2i

https://doi.org/10.5194/egusphere-2026-622
Preprint. Discussion started: 12 February 2026


platform, and the ENVITOP platform. We also thanks Helge A. Winkelbauer for providing global iodine speciation dataset, and Rosalind E.M. Rickaby for the inspiring discussions on the topic.

**Financial support**

**References**

Allen, K.A., Hönisch, B., Eggins, S.M., Haynes, L.L., Rosenthal, Y., Yu, J., 2016. Trace element proxies for surface ocean conditions: A synthesis of culture calibrations with planktic foraminifera. Geochim. Cosmochim. Acta 193, 197–221. https://doi.org/10.1016/j.gca.2016.08.015

Bard, E., Ménot, G., Rostek, F., Licari, L., Böning, P., Edwards, R.L., Cheng, H., Wang, Y., Heaton, T.J., 2013. Radiocarbon Calibration/Comparison Records Based on Marine Sediments from the Pakistan and Iberian Margins. Radiocarbon 55, 1999–2019. https://doi.org/10.2458/azu_js_rc.55.17114

Barker, S., Greaves, M., Elderfield, H., 2003. A study of cleaning procedures used for foraminiferal Mg/Ca paleothermometry: MG/CA PALEOTHERMOMETRY. Geochem. Geophys. Geosystems 4, n/a-n/a. https://doi.org/10.1029/2003GC000559

Behrenfeld, M.J., Falkowski, P.G., 1997. Photosynthetic rates derived from satellite-based chlorophyll concentration. Limnol. Oceanogr. 42, 1–20. https://doi.org/10.4319/lo.1997.42.1.0001

Bopp, L., Resplandy, L., Orr, J.C., Doney, S.C., Dunne, J.P., Gehlen, M., Halloran, P., Heinze, C., Ilyina, T., Séférian, R., Tjiputra, J., Vichi, M., 2013. Multiple stressors of ocean ecosystems in the 21st century: projections with CMIP5 models. Biogeosciences 10, 6225–6245. https://doi.org/10.5194/bg-10-6225-2013

Boussetta, S., Bassinot, F., Sabbatini, A., Caillon, N., Nouet, J., Kallel, N., Rebaubier, H., Klinkhammer, G., Labeyrie, L., 2011. Diagenetic Mg-rich calcite in Mediterranean sediments: Quantification and impact on foraminiferal Mg/Ca thermometry. Mar. Geol. 280, 195–204. https://doi.org/10.1016/j.margeo.2010.12.011

Chai, J.Y., Muramatsu, Y., 2007. Determination of Bromine and Iodine in Twenty-three Geochemical Reference Materials by ICP-MS. Geostand. Geoanalytical Res. 31, 143–150. https://doi.org/10.1111/j.1751-908X.2007.00856.x

Chance, R., Baker, A.R., Carpenter, L., Jickells, T.D., 2014. The distribution of iodide at the sea surface. Env. Sci Process. Impacts 16, 1841–1859. https://doi.org/10.1039/C4EM00139G

Chance, R., Weston, K., Baker, A.R., Hughes, C., Malin, G., Carpenter, L., Meredith, M.P., Clarke, A., Jickells, T.D., Mann, P., Rossetti, H., 2010. Seasonal and interannual variation of dissolved iodine speciation at a coastal Antarctic site. Mar. Chem. 118, 171–181. https://doi.org/10.1016/j.marchem.2009.11.009

Chance, R.J., Tinel, L., Sherwen, T., Baker, A.R., Bell, T., Brindle, J., Campos, M.L.A.M., Croot, P., Ducklow, H., Peng, H., Hopkins, F., Hoogakker, B., Hughes, C., Jickells, T.D., Loades, D., Macaya, D.A.R., Mahajan, A.S., Malin, G., Phillips, D., Roberts, I., Roy, R., Sarkar, A., Sinha, A.K., Song, X., Winkelbauer, H., Wuttig, K., Yang, M., Peng, Z., Carpenter, L.J., 2019. Global sea-surface iodide observations, 1967–2018. Sci. Data 6, 286. https://doi.org/10.1038/s41597-019-0288-y

Cornuault, M., Tachikawa, K., Vidal, L., Guihou, A., Siani, G., Deschamps, P., Bassinot, F., Revel, M., 2018. Circulation Changes in the Eastern Mediterranean Sea Over the Past 23,000 Years Inferred From Authigenic Nd Isotopic Ratios. Paleoceanogr. Paleoclimatology 33, 264–280. https://doi.org/10.1002/2017PA003227

Crudeli, D., Young, J.R., Erba, E., De Lange, G.J., Henriksen, K., Kinkel, H., Slomp, C.P., Ziveri, P., 2004. Abnormal carbonate diagenesis in Holocene–late Pleistocene sapropel-associated sediments from the Eastern Mediterranean; evidence from Emiliania huxleyi coccolith morphology. Mar. Micropaleontol. 52, 217–240. https://doi.org/10.1016/j.marmicro.2004.04.010

Elderfield, H., Truesdale, V.W., 1980. On the biophilic nature of iodine in seawater. Earth Planet. Sci. Lett. 50, 105–114. https://doi.org/10.1016/0012-821X(80)90122-3

Eynaud, F., De Abreu, L., Voelker, A., Schönfeld, J., Salgueiro, E., Turon, J., Penaud, A., Toucanne, S., Naughton, F., Sánchez Goñi, M.F., Malaizé, B., Cacho, I., 2009. Position of the Polar Front along the western Iberian margin during key cold episodes of the last 45 ka. Geochem. Geophys. Geosystems 10, 2009GC002398. https://doi.org/10.1029/2009GC002398

Feng, X., Redfern, S.A.T., 2018. Iodate in calcite, aragonite and vaterite CaCO3: Insights from first-principles calculations and implications for the I/Ca geochemical proxy. Geochim. Cosmochim. Acta 236, 351–360. https://doi.org/10.1016/j.gca.2018.02.017

Frölicher, T.L., Rodgers, K.B., Stock, C.A., Cheung, W.W.L., 2016. Sources of uncertainties in 21st century projections of potential ocean ecosystem stressors. Glob. Biogeochem. Cycles 30, 1224–1243. https://doi.org/10.1002/2015GB005338

https://doi.org/10.5194/egusphere-2026-622
Preprint. Discussion started: 12 February 2026


Global Ocean Physics Reanalysis [WWW Document], 2025. . Copernic. Mar. Data. https://doi.org/10.48670/moi-00021

Hepach, H., Hughes, C., Hogg, K., Collings, S., Chance, R., 2020. Senescence as the main driver of iodide release from a diverse range of marine phytoplankton. Biogeosciences 17, 2453–2471. https://doi.org/10.5194/bg-17-2453-2020

Hess, A.V., Rosenthal, Y., Zhou, X., Bu, K., 2025. The I/Ca paleo-oxygenation proxy in planktonic foraminifera: A multispecies core-top calibration. Geochim. Cosmochim. Acta S0016703725000298. https://doi.org/10.1016/j.gca.2025.01.018

Hönisch, B., Bijma, J., Russell, A.D., Spero, H.J., Palmer, M.R., Zeebe, R.E., Eisenhauer, A., 2003. The influence of symbiont photosynthesis on the boron isotopic composition of foraminifera shells. Mar. Micropaleontol. 49, 87–96. https://doi.org/10.1016/S0377-8398(03)00030-6

Hoogakker, B., Davis, C., Wang, Y., Kusch, S., Nilsson-Kerr, K., Hardisty, D., Jacobel, A., Reyes Macaya, D., Glock, N., Ni, S., Sepúlveda, J., Ren, A., Auderset, A., Hess, A., Meissner, K., Cardich, J., Anderson, R., Barras, C., Basak, C., Bradbury, H., Brinkmann, I., Castillo, A., Cook, M., Costa, K., Choquel, C., Diz, P., Donnenfield, J., Elling, F., Erdem, Z., Filipsson, H., Garrido, S., Gottschalk, J., Govindankutty Menon, A., Groeneveld, J., Hallman, C., Hendy, I., Hennekam, R., Lu, W., Lynch-Stieglitz, J., Matos, L., Martínez-García, A., Molina, G., Muñoz, P., Moretti, S., Morford, J., Nuber, S., Radionovskaya, S., Raven, M., Somes, C., Studer, A., Tachikawa, K., Tapia, R., Tetard, M., Vollmer, T., Wu, S., Zhang, Y., Zheng, X.-Y., Zhou, Y., 2024. Reviews and syntheses: Review of proxies for low-oxygen paleoceanographic reconstructions. https://doi.org/10.5194/egusphere-2023-2981

Jickells, T.D., Boyd, S.S., Knap, A.H., 1988. Iodine cycling in the Sargasso Sea and the Bermuda inshore waters. Mar. Chem. 24, 61–82. https://doi.org/10.1016/0304-4203(88)90006-0

Jones, M.R., Chance, R., Bell, T., Jones, O., Loades, D.C., May, R., Tinel, L., Weddell, K., Widdicombe, C., Carpenter, L.J., 2024. Iodide, iodate & dissolved organic iodine in the temperate coastal ocean. Front. Mar. Sci. 11, 1277595. https://doi.org/10.3389/fmars.2024.1277595

Lu, W., Dickson, A.J., Thomas, E., Rickaby, R.E.M., Chapman, P., Lu, Z., 2020. Refining the planktic foraminiferal I/Ca proxy: Results from the Southeast Atlantic Ocean. Geochim. Cosmochim. Acta 287, 318–327. https://doi.org/10.1016/j.gca.2019.10.025

Lu, Z., Hoogakker, B.A.A., Hillenbrand, C.-D., Zhou, X., Thomas, E., Gutchess, K.M., Lu, W., Jones, L., Rickaby, R.E.M., 2016. Oxygen depletion recorded in upper waters of the glacial Southern Ocean. Nat. Commun. 9.

Lu, Z., Jenkyns, H.C., Rickaby, R.E.M., 2010. Iodine to calcium ratios in marine carbonate as a paleo-redox proxy during oceanic anoxic events. Geology 38, 1107–1110. https://doi.org/10.1130/G31145.1

Luther, G.W., 2023. Review on the physical chemistry of iodine transformations in the oceans. Front. Mar. Sci. 10, 1085618. https://doi.org/10.3389/fmars.2023.1085618

Martrat, B., Grimalt, J.O., Lopez-Martinez, C., Cacho, I., Sierro, F.J., Flores, J.A., Zahn, R., Canals, M., Curtis, J.H., Hodell, D.A., 2004. Abrupt Temperature Changes in the Western Mediterranean over the Past 250,000 Years. Science 306, 1762–1765. https://doi.org/10.1126/science.1101706

Meister, P., Herda, G., Petrishcheva, E., Gier, S., Dickens, G.R., Bauer, C., Liu, B., 2022. Microbial Alkalinity Production and Silicate Alteration in Methane Charged Marine Sediments: Implications for Porewater Chemistry and Diagenetic Carbonate Formation. Front. Earth Sci. 9, 756591. https://doi.org/10.3389/feart.2021.756591

Mishonov, A.V., Boyer, T.P., Baranova, O.K., Bouchard, C.N., Cross, S.L., Garcia, H.E., Locarnini, R.A., Paver, C.R., Reagan, J.R., Wang, Z., Seidov, D., Grodsky, A.I., Beauchamp, J.G., 2024. World Ocean Database 2023 [WWW Document]. https://doi.org/10.25923/z885-h264

Nilsson-Kerr, K., Hoogakker, B.A.A., Macaya, D.A.R., Winkelbauer, H.A., Hamilton, E., Chenery, S., Davis, C.V., Leng, M.J., 2025. Late Cenozoic intensification of deoxygenation in the Pacific Ocean. Earth Planet. Sci. Lett. 655, 119253. https://doi.org/10.1016/j.epsl.2025.119253

Oregon State University ORCA, n.d. ORCA Science [WWW Document]. Or. State Univ. ORCA. URL http://orca.science.oregonstate.edu/index.php (accessed 6.17.25).

Oschlies, A., Brandt, P., Stramma, L., Schmidtko, S., 2018. Drivers and mechanisms of ocean deoxygenation. Nat. Geosci. 11, 467–473. https://doi.org/10.1038/s41561-018-0152-2

Oschlies, A., Duteil, O., Getzlaff, J., Koeve, W., Landolfi, A., Schmidtko, S., 2017. Patterns of deoxygenation: sensitivity to natural and anthropogenic drivers. Philos. Trans. R. Soc. Math. Phys. Eng. Sci. 375, 20160325. https://doi.org/10.1098/rsta.2016.0325

Packard, T.T., Minas, H.J., Coste, B., Martinez, R., Bonin, M.C., Gostan, J., Garfield, P., Christensen, J., Dortch, Q., Minas, M., Copin-Montegut, G., Copin-Montegut, C., 1988. Formation of the Alboran oxygen minimum zone. Deep Sea Res. Part Oceanogr. Res. Pap. 35, 1111–1118. https://doi.org/10.1016/0198-0149(88)90003-9

https://doi.org/10.5194/egusphere-2026-622
Preprint. Discussion started: 12 February 2026


Pichevin, L., Bard, E., Martinez, P., Billy, I., 2007. Evidence of ventilation changes in the Arabian Sea during the late Quaternary: Implication for denitrification and nitrous oxide emission. Glob. Biogeochem. Cycles 21, 2006GB002852. https://doi.org/10.1029/2006GB002852

Podder, J., Lin, J., Sun, W., Botis, S.M., Tse, J., Chen, N., Hu, Y., Li, D., Seaman, J., Pan, Y., 2017. Iodate in calcite and vaterite: Insights from synchrotron X-ray absorption spectroscopy and first-principles calculations. Geochim. Cosmochim. Acta 198, 218–228. https://doi.org/10.1016/j.gca.2016.11.032

Powley, H.R., Cappellen, P.V., Krom, M.D., 2017. Nutrient Cycling in the Mediterranean Sea: The Key to Understanding How the Unique Marine Ecosystem Functions and Responds to Anthropogenic Pressures, in: Fuerst-Bjelis, B. (Ed.), Mediterranean Identities - Environment, Society, Culture. InTech. https://doi.org/10.5772/intechopen.70878

Ram, S., Erez, J., 2023. Anion elements incorporation into corals skeletons: Experimental approach for biomineralization and paleo-proxies. Proc. Natl. Acad. Sci. 120, e2306627120. https://doi.org/10.1073/pnas.2306627120

Schlitzer, Reiner, 2025. Ocean Data View [WWW Document]. Ocean Data View. URL https://odv.awi.de/ (accessed 12.10.25).

Schneider, A., Wallace, D.W.R., Körtzinger, A., 2007. Alkalinity of the Mediterranean Sea. Geophys. Res. Lett. 34, 2006GL028842. https://doi.org/10.1029/2006GL028842

Siani, G., Paterne, M., Colin, C., 2010. Late glacial to Holocene planktic foraminifera bioevents and climatic record in the South Adriatic Sea. J. Quat. Sci. 25, 808–821. https://doi.org/10.1002/jqs.1360

Suess, E., 1979. Mineral phases formed in anoxic sediments by microbial decomposition of organic matter. Geochim. Cosmochim. Acta 43, 339–352. https://doi.org/10.1016/0016-7037(79)90199-6

Tian, R.C., Nicolas, E., 1995. Iodine speciation in the northwestern Mediterranean Sea, method and vertical profile. Mar. Chem. 48, 151–156. https://doi.org/10.1016/0304-4203(94)00048-I

Ullman, W.J., Luther, G.W., de Lange, G.J, Woittiez, J.R.W, 1990. Iodine chemistry in deep anoxic basins and overlying waters of the Mediterranean Sea.

Wadley, M.R., Stevens, D.P., Jickells, T.D., Hughes, C., Chance, R., Hepach, H., Tinel, L., Carpenter, L.J., 2020. A Global Model for Iodine Speciation in the Upper Ocean. Glob. Biogeochem. Cycles 34, e2019GB006467. https://doi.org/10.1029/2019GB006467

Winkelbauer, H., Cordova-Rodriguez, K., Reyes-Macaya, D., Scott, J., Glock, N., Lu, Z., Hamilton, E., Chenery, S., Holdship, P., Dormon, C., Hoogakker, B., 2021. Foraminifera Iodine to Calcium Ratios: Approach and Cleaning. Geochem. Geophys. Geosystems 22. https://doi.org/10.1029/2021GC009811

Winkelbauer, H.A., Hoogakker, B.A.A., Chance, R.J., Davis, C.V., Anthony, C.J., Bischoff, J., Carpenter, L.J., Chenery, S.R.N., Hamilton, E.M., Holdship, P., Peck, V.L., Poulton, A.J., Stinchcombe, M.C., Wishner, K.F., 2023. Planktic foraminifera iodine/calcium ratios from plankton tows. Front. Mar. Sci. 10, 1095570. https://doi.org/10.3389/fmars.2023.1095570

Wong, G.T.F., Zhang, L., 1992. Changes in iodine speciation across coastal hydrographic fronts in southeastern United States continental shelf waters. Cont. Shelf Res. 12, 717–733. https://doi.org/10.1016/0278-4343(92)90027-H

Zhou, X., Hess, A.V., Bu, K., Sagawa, T., Rosenthal, Y., 2022. Simultaneous Determination of I/Ca and Other Elemental Ratios in Foraminifera: Comparing Results From Acidic and Basic Solutions. Geochem. Geophys. Geosystems 23, e2022GC010660. https://doi.org/10.1029/2022GC010660

Zhou, X., Thomas, E., Rickaby, R.E.M., Winguth, A.M.E., Lu, Z., 2014. I/Ca evidence for upper ocean deoxygenation during the PETM. Paleoceanography 29, 964–975. https://doi.org/10.1002/2014PA002702